Anisotropic in-plane reversible strain effect in $Y_{0.5}Gd_{0.5}Ba_2Cu_3O_{7-\delta}$ coated conductors

2011 Supercond. Sci. Technol. 24 115010

(http://iopscience.iop.org/0953-2048/24/11/115010)

Supercond. Sci. Technol. **24** (2011) 115010 (8pp) doi:10.1088/0953-2048/24/11/115010

Anisotropic in-plane reversible strain effect in $Y_{0.5}Gd_{0.5}Ba_2Cu_3O_{7-\delta}$ coated conductors*

D C van der Laan[1,2], D Abraimov[3], A A Polyanskii[3], D C Larbalestier[3], J F Douglas[2,5], R Semerad[4] and M Bauer[4]

[1] Department of Physics, University of Colorado, Boulder, CO 80309, USA
[2] National Institute of Standards and Technology, Boulder, CO 80305, USA
[3] Applied Superconductivity Center, National High Magnetic Field Laboratory, Florida State University, Tallahassee, FL 32310, USA
[4] THEVA Dünnschichttechnik GMBH, D-85737, Ismaning, Germany

E-mail: danko@boulder.nist.gov

Received 16 August 2011, in final form 20 September 2011
Published 19 October 2011
Online at stacks.iop.org/SUST/24/115010

Abstract
Recent experiments have shown that reversible effects of strain on the critical current density and flux pinning strength in the high-temperature superconductor $Bi_2Sr_2Ca_2Cu_3O_x$ can be explained entirely by the pressure dependence of its critical temperature. Such a correlation is less simple for RE–$Ba_2Cu_3O_{7-\delta}$ (RE = rare earth) superconductors, in part because the in-plane pressure dependence of its critical temperature is highly anisotropic. Here, we make a qualitative correlation between the uniaxial pressure dependence of the critical temperature and the reversible strain effect on the critical current of RE–$Ba_2Cu_3O_{7-\delta}$ coated conductors by taking the crystallography and texture of the superconducting film into account. The strain sensitivity of the critical current is highest when strain is oriented along the [100] and [010] directions of the superconducting film, whereas the critical current becomes almost independent of strain when strain is oriented along the [110] direction. The results confirm the important role of the anisotropic pressure dependence of the critical temperature on the reversible strain behavior of RE–$Ba_2Cu_3O_{7-\delta}$. The reversible strain effect in RE–$Ba_2Cu_3O_{7-\delta}$ is expected to decrease the performance of the conductor in many applications, such as high-field magnets, but the effect may be only minor in coated conductor cables, where strain is generally not aligned with the tape axis.

1. Introduction

Axial strain irreversibly degrades the critical current (I_c) of high-temperature superconducting tapes and wires when it exceeds the irreversible strain limit and the conductor is damaged mechanically [1–4]. Strain affects the critical current density (J_c) and flux pinning strength of $Bi_2Sr_2CaCu_2O_x$ (Bi-2212) wires and tapes [5], $Bi_2Sr_2Ca_2Cu_3O_x$ (Bi-2223) tapes [6–9], and RE–$Ba_2Cu_3O_{7-\delta}$ (RE = Y, Gd, Dy, Sm, etc) (REBCO) coated conductors [10–17], even before damage to the superconductor occurs. This change is fully reversible, which means that I_c and the flux pinning strength return to their initial value after the strain has been released. Recent work rules out that the reversible strain effect originates from grain boundaries where dislocations may obstruct the grain boundary supercurrent [18, 19]. Instead, in the case of Bi-2223 tapes, the linear change in I_c with strain and the strain dependence of the flux pinning force can be entirely explained by the pressure dependence of the critical temperature (T_c) [9]. Although the strain dependence of I_c in most REBCO coated conductors is approximately parabolic, it is linear in coated conductors that are fabricated with the inclined-substrate deposition (ISD) method. Similar to Bi-2223, the linear, reversible strain dependence of both I_c and T_c suggests a correlation between the two for ISD REBCO coated conductors [20, 21].

A closer investigation into the microstructure of REBCO coated conductors is needed to fully correlate the uniaxial

* Contribution of NIST, not subject to US copyright.
[5] Present address: Intel Corp., Portland, OR, USA.

Table 1. Properties of REBCO samples.

Sample #	Superconducting film	Template	Tape width (mm)	J_c (MA cm^{-2}) 76 K, self-field
S-1	$GdBa_2Cu_3O_{7-\delta}$	IBAD-MOCVD	4	2.5
S-2	$YBa_2Cu_3O_{7-\delta}$	IBAD-MOCVD	4	3.0
S-3	$Gd_{0.5}Y_{0.5}Ba_2Cu_3O_{7-\delta}$	IBAD-MOCVD	12	2.5
S-4	$DyBa_2Cu_3O_{7-\delta}$	ISD	4	1.8

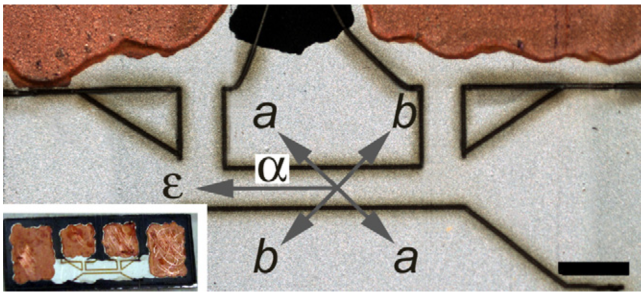

Figure 1. Optical image of one of the bridges that was patterned by laser in sample S-3. The bridge is 1 mm long and 200 μm wide. The remaining copper on the pads where the voltage contacts was soldered is visible in the top part of the image. The black lines are the laser cuts. The arrows show how the alignment of the bridge with the *a*- and *b*-axes of the twinned superconducting film defines the angle α. The inset at the lower left corner shows the entire sample, including the copper contact pads. The scale bar on the left is 300 μm.

(This figure is in colour only in the electronic version)

pressure dependence of T_c and the reversible strain effect on I_c. Such a correlation is more difficult to make in REBCO compared to Bi-2223, since the in-plane pressure dependence of T_c in REBCO is highly anisotropic [22], while it is fully isotropic in Bi-2212 and Bi-2223 [23–25]. Here, we correlate the microstructure, pressure dependence of T_c and reversible strain effect on I_c in REBCO coated conductors. We also demonstrate that the combination of the anisotropic in-plane pressure dependence of T_c and the high degree of texture in these materials results in an anisotropic in-plane reversible strain effect on I_c. The specific crystallographic orientation dependence of the properties turns out to be very beneficial for the construction of a new cable type, since it is possible to arrange the principal strain along the least sensitive axis.

2. Experiment

The effect of strain on the critical current was measured on several types of REBCO coated conductors (see table 1). Samples S-1, S-2 and S-3 were $GdBa_2Cu_3O_{7-\delta}$ (GBCO), $YBa_2Cu_3O_{7-\delta}$ (YBCO) and $Y_{0.5}Gd_{0.5}Ba_2Cu_3O_{7-\delta}$ (YGBCO) coated conductors, respectively deposited on a 50 μm thick Hastelloy C-276 substrate using an ion-beam-assisted deposition (IBAD) template. The 1 μm thick REBCO superconducting layer was deposited on top of the buffer layers by metal–organic chemical-vapor deposition (MOCVD) [26, 27]. Such a deposition route results in a twinned superconducting film that is oriented with the [100] and [010] directions along the tape axis [28]. A silver cap layer, 2–3 μm thick, was deposited on top of the superconducting layer. Some of the coated conductors were slit from a 12 mm wide tape to their final width of 4 mm, and all samples were surround-plated with 20 μm of copper for electrical and thermal stability.

Table 2. Parameter values used in equation (1).

Sample #	α (deg)	$I_c(\varepsilon_m)$ (A)	a (%$^{-1}$)	ε_m (%)
S-1	0	97.4	4667	−0.04
S-2	0	137.3	9378	0.11
B-1	1.1	4.91	7705	0.03
B-2	1.0	4.98	7647	0.06
B-3	22.7	3.25	4783	0.03
B-4	21.9	4.70	4744	0.02
B-5	44.7	5.13	259	−0.67
B-6	47.4	5.26	580	−0.39
B-7	65.1	5.18	4045	0.05
B-8	67.5	0.57	—	—
B-9	69.8	—	—	—
B-10	89.0	4.92	7745	0.10
B-11	88.2	4.54	8866	0.08
B-12	88.3	0.73	—	—

Sample S-4 was a 1 μm thick $DyBa_2Cu_3O_{7-\delta}$ (DBCO) film that was deposited on an ISD MgO template [29]. A silver cap layer, 10 μm thick, was deposited on top of the superconducting layer. The twinned superconducting film that was deposited on the ISD template is aligned with the [110] direction along the tape axis [30], which makes a distinct contrast to the MOCVD conductors in which the [100] or [010] direction tends to be aligned along the tape axis.

Superconducting bridges were prepared from sample S-3 by cutting sections 12 mm long and 5 mm wide from the 12 mm wide conductor at specific angles with respect to the conductor axis. Wet chemical etching was used to remove most of the copper, except in locations where current and voltage contacts needed to be soldered. The contact pad areas were manually painted with GE-7031 varnish and the copper layer was etched with a solution of 15–20% ammonium persulfate and 75–80% water for 25–30 min at room temperature. Part of the silver cap layer was removed by etching with a solution of ammonia water and hydrogen peroxide. A single bridge, 1 mm in length and 200 μm in width, was automatically patterned through the silver and superconducting layers with a Nd–YAG laser on each of the cut pieces (see figure 1). A total of 12 bridges (samples B-1 to B-12; see table 2 below) were patterned at specific angles α, with respect to the axis of the original tape, ranging from 0° (parallel to the tape axis) to 90° (perpendicular to the tape axis). The orientation of the bridge was measured after patterning with an uncertainty in α of about ±0.5°. The critical current density of the laser patterned bridges was within 75% of that of the original 12 mm wide conductor.

The coated conductors used to pattern the bridges contain local defects that predominantly run along the length of the

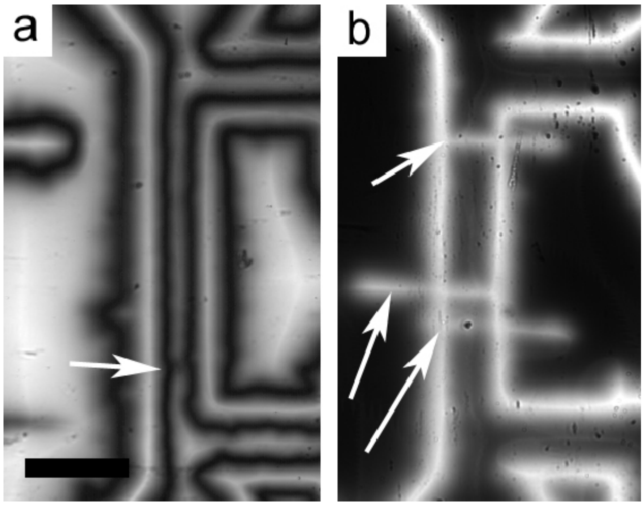

Figure 2. (a) Magneto-optical image of sample B-11 taken after the sample was field-cooled to 7 K in a field of 120 mT. The image shows a small defect, indicated by the arrow, running across the bridge width. (b) Magneto-optical image of sample B-12 taken at 60 mT, after the sample was cooled in zero field to 7 K, showing easy magnetic flux penetration along three large defects running across the bridge width, indicated by the arrows. The scale bar on the left is 300 μm.

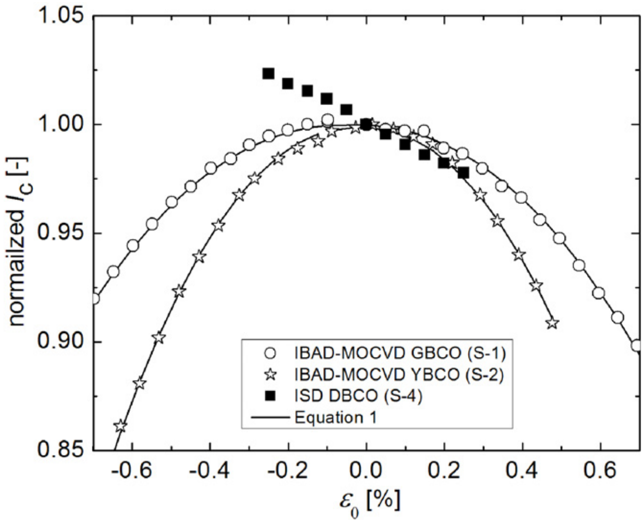

Figure 3. Normalized critical current as a function of intrinsic strain at 76 K for IBAD-MOCVD GBCO sample S-1, IBAD-MOCVD YBCO sample S-2, and as a function of applied strain for ISD DBCO sample S-4. The data shown are fully reversible. The solid lines are fits to the data according to equation (1).

conductor and are related to mechanical defects in the substrate or buffer layers [31–35]. Such defects sometimes cross the patterned bridge, which severely lowers the I_c (for instance in samples B-8, B-9, and B-12; see table 2). The presence of local defects was detected by magneto-optical imaging, which shows local flux penetration through defects within the films (see figure 2). An example of a smaller defect in sample B-11 that does not affect the critical current is shown in figure 2(a), whereas much larger defects that cross the bridge in sample B-12 and limit its critical current are shown in figure 2(b).

The dependence of the critical current on axial strain of the coated conductors and coated conductor bridges was measured at 76 K. The samples were soldered onto the surface of a 98 wt% Cu–2 wt% Be (CuBe) bending beam by use of 52 wt% In–48 wt% Sn solder with a melting temperature of 118 °C. Axial strain was applied along the length of the coated conductor bridges, with an uncertainty in strain alignment of about ±2°, by bending the beam in a four-point bender [15]. The critical current was determined with a four-contact measurement with an uncertainty of about ±0.3% at an electric-field criterion of 1 μV cm^{-1}. Strain was measured directly with a strain gage mounted on top of the beam.

3. Results and discussion

3.1. Reversible effect of strain on I_c in REBCO coated conductors

Typical dependences of the critical current of REBCO coated conductors on strain are presented in figure 3. The normalized I_c, as a function of intrinsic strain ε_0, is shown for three conductors. IBAD-MOCVD samples S-1 and S-2 show an almost parabolic strain dependence of I_c with a clear maximum, while the sample that was manufactured by use of the ISD process (sample S-4) shows a linear strain dependence of I_c. The intrinsic strain is the strain in the superconducting film and depends on pre-strain caused by the mismatch in thermal contraction between the various components of the conductor: $\varepsilon_0 \equiv \varepsilon - \varepsilon_m$ [15, 36]. The superconducting film is under the optimum strain state at a strain ε_m at which the peak in I_c is reached. The critical currents, as shown in figure 3, are normalized to their peak values for IBAD-MOCVD samples S-1 and S-2, while I_c of the ISD sample S-4 is normalized to its value at zero strain. The intrinsic strain of the ISD sample S-4 is unknown, because the optimum strain state cannot be determined from its linear strain dependence. The critical current of sample S-4 is therefore plotted as a function of applied strain. The change in I_c with strain is fully reversible in all three samples over the range of strain shown, which was confirmed by a full recovery of I_c after the strain has been released (not shown).

The power-law strain dependence of the critical current in IBAD-MOCVD conductors is often described with the following fitting function [15–17]:

$$I_c(\varepsilon, \alpha) = I_c(\varepsilon_m)(1 - a(\alpha)|\varepsilon - \varepsilon_m(\alpha)|^{2.18}), \qquad (1)$$

where the parameter a represents the strain sensitivity of I_c and $I_c(\varepsilon_m)$ is the maximum critical current at an applied strain ε_m. The expansion of equation (1) by adding the angular dependence, with α defined as the angle between the strain and the a- and b-axes of the superconducting film, will be discussed below. The main difference between the two IBAD-MOCVD samples (S-1 and S-2) is that the strain sensitivity of I_c for $GdBa_2Cu_3O_{7-\delta}$ sample S-1 is only about 57% of that of $YBa_2Cu_3O_{7-\delta}$ sample S-2 (see table 2) [37]. Such a large difference in strain sensitivity could be caused by differences between $GdBa_2Cu_3O_{7-\delta}$ and $YBa_2Cu_3O_{7-\delta}$ in the uniaxial pressure dependences of T_c, but also by differences in microstructure, as will be discussed in section 3.2.

3.2. Influence of the crystallographic texture on the reversible strain effect

The pressure dependence of T_c in Bi-2212 and Bi-2223 is fully isotropic within the *ab*-plane: T_c increases linearly with pressure applied along the *a*- and *b*-axes at the same rate [23–25]. Because of this isotropic in-plane pressure dependence, and the fact that a macroscopic transport current runs predominantly within the *ab*-planes, microstructural features, such as grain boundaries and grain orientation, do not influence the reversible strain effect on I_c and on the flux pinning strength measured in Bi-2223 tapes. Although T_c most likely varies locally within the microstructure, its relative change with in-plane strain is the same throughout the microstructure, and thus a quantitative correlation between the reversible strain effect and the pressure dependence of T_c in Bi-2223 tapes could be made [9].

On the other hand, the superconducting microstructure needs to be taken into account to make a direct correlation between the pressure dependence of T_c and the macroscopic reversible strain effect on I_c in REBCO coated conductors. The change in T_c with uniaxial pressure in REBCO high-temperature superconductors is highly anisotropic within the *ab*-plane: T_c increases linearly with pressure applied along the *b*-axis, whereas it decreases at the same rate when pressure is applied along the *a*-axis [22]. We will ignore the *c*-axis pressure component of T_c in the remainder of this work, since only a minor decrease in T_c with pressure is measured when pressure is applied along the *c*-axis, and the lattice deformation in our experiment occurs predominantly within the *ab*-plane.

Twin planes within the microstructures of REBCO superconductors, such as in YBCO and GBCO, cause the anisotropic in-plane pressure dependence of T_c to play a major role in the reversible strain dependence of I_c. The superconducting grains in IBAD-MOCVD coated conductors are aligned with their *a*- and *b*-axes along the conductor axis, as has been shown in synchrotron studies [28]. Twin planes at which the lattice of the superconducting film rotates in-plane by 90°, and which are generally oriented at 45° to the *a*- and *b*-axes of the film [38, 39], cause a local switching between the [100] and [010] directions along the coated conductor axis. Strain applied along the conductor axis is thus locally orientated along either the *a*-axis or along the *b*-axis of the superconducting film (see figure 4(a)). The stress thus causes either a local linear increase, or local decrease, in T_c, and thus I_c, on either side of each twin boundary. An optimum strain state exists in which the macroscopic I_c is maximum, and where the overall distribution in T_c (and thus I_c) in the conductor is lowest. Any deviation from the optimum strain state will cause local dissipation to increase as the twin plane is crossed into a domain with reduced T_c, which in turn will reduce the overall critical current. The voltage generated by a macroscopic transport current over the two domains outlined in figure 4(a) is given by

$$V_{\mathrm{tot}}(I,\varepsilon_0) = V_{\mathrm{c,tot}}\left(\frac{I}{I_{\mathrm{c,tot}}(\varepsilon_0)}\right)^n = V_1(I,\varepsilon_0) + V_2(I,\varepsilon_0)$$
$$= V_{\mathrm{c},1}\left(\frac{I}{I_{\mathrm{c},1}(\varepsilon_0)}\right)^n + V_{\mathrm{c},2}\left(\frac{I}{I_{\mathrm{c},2}(\varepsilon_0)}\right)^n, \qquad (2a)$$

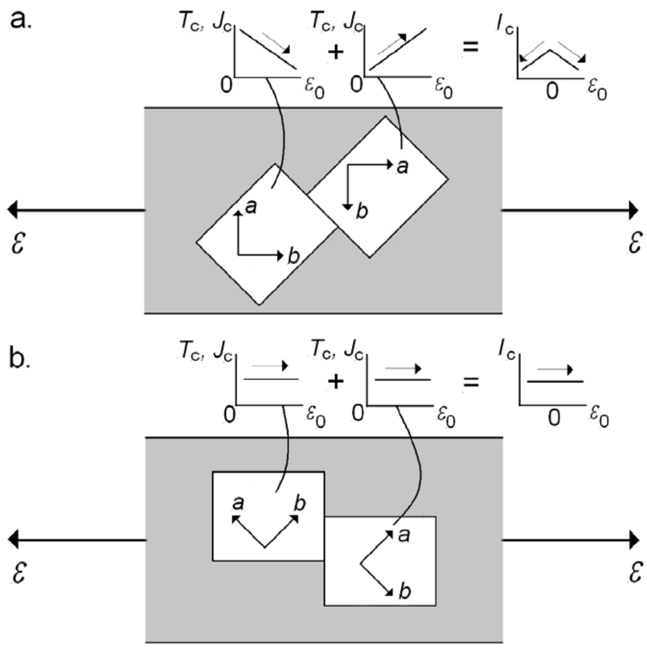

Figure 4. (a) Representation of two domains of 90° rotation across a twin boundary in an IBAD-MOCVD REBCO coated conductor. The twin boundaries are oriented at 45° to the *a*- and *b*-axes of the superconducting film. The linear change in T_c and J_c with strain that is applied along the conductor axis is indicated on each side of the twin boundary, together with the strain dependence of $I_{\mathrm{c,tot}}$ of both domains in series, as defined by equation (4). (b) Representation of two domains of 90° rotation across a twin boundary in an ISD DBCO coated conductor with the strain applied along the [110] direction of the superconducting film.

with the temperature dependence of the critical current of each domain given by [40]:

$$I_{\mathrm{c},1}(T,\varepsilon_0) = I_{\mathrm{c},1}(0,0)\left(1 - \frac{T}{T_{\mathrm{c},1}(\varepsilon_0)}\right)^{1.5}$$
$$= I_{\mathrm{c},1}(0,0)\left(1 - \frac{75.9}{-b\varepsilon_0 + T_{\mathrm{c}}(0)}\right)^{1.5} \qquad (2b)$$

and

$$I_{\mathrm{c},2}(T,\varepsilon_0) = I_{\mathrm{c},2}(0,0)\left(1 - \frac{T}{T_{\mathrm{c},2}(\varepsilon_0)}\right)^{1.5}$$
$$= I_{\mathrm{c},2}(0,0)\left(1 - \frac{75.9}{b\varepsilon_0 + T_{\mathrm{c}(0)}}\right)^{1.5}. \qquad (2c)$$

Here, V_1 and V_2 are the voltages generated across domains 1 and 2 on either side of the twin plane that depend on the strain and temperature-dependent critical currents $I_{\mathrm{c},1}(T,\varepsilon)$ and $I_{\mathrm{c},2}(T,\varepsilon)$. The strain dependence of I_c across the twin plane is caused entirely by the change in T_c with strain at the rate indicated by parameter *b*, which is expected to be around 4 K/%, based on the in-plane elastic modulus of 189 GPa for YBCO [41]. The *n*-value, which determines the steepness of the superconducting transition, is assumed to be the same for each grain on either side of each twin plane, and $I_{\mathrm{c},1}(0,0) = I_{\mathrm{c},2}(0,0)$. Also, when both domains on either side of the twin plane are equal in size, the voltage at the criterion that determines I_c is: $V_{\mathrm{c,tot}} = 2V_{\mathrm{c},1} = 2V_{\mathrm{c},2}$. With these approximations, both sides of equation (2*a*) can be rewritten as

$$V_{\mathrm{tot}}(I,\varepsilon_0) = 2V_{\mathrm{c},1}\left(\frac{I}{I_{\mathrm{c,tot}}(\varepsilon_0)}\right)^n$$

$$= V_{\mathrm{c},1}\left(\left(\frac{I}{I_{\mathrm{c},1}(\varepsilon_0)}\right)^n + \left(\frac{I}{I_{\mathrm{c},2}(\varepsilon_0)}\right)^n\right). \quad (3)$$

The strain dependence of the total critical current $I_{\mathrm{c,tot}}(\varepsilon)$ of both domains in series can be obtained from equation (3) and is given by:

$$I_{\mathrm{c,tot}}(\varepsilon_0) = I_{\mathrm{c},1}(\varepsilon_0)I_{\mathrm{c},2}(\varepsilon_0)\left(\frac{2}{I^n_{\mathrm{c},1}(\varepsilon_0) + I^n_{\mathrm{c},2}(\varepsilon_0)}\right)^{\frac{1}{n}}. \quad (4)$$

The strain dependence of T_{c} and I_{c} of individually oriented domains and that of $I_{\mathrm{c,tot}}$ are outlined in more detail in figure 4(a) for the simplified case of two domains with switched orientation in series. The linear strain dependence of T_{c} will result in a near-linear strain dependence of I_{c} in each domain across the twin plane and a rounded rooftop-like strain dependence of the overall $I_{\mathrm{c,tot}}$, with a peak in $I_{\mathrm{c,tot}}$ at the optimum strain ε_{m} ($\varepsilon_0 = 0$), defined by equation (4).

Earlier studies showed that low-angle grain boundaries in REBCO films have a different strain state from the grains and thus have a different T_{c} compared to the grains [18, 19], which adds to the overall distribution in T_{c} within these films. Still, T_{c} of the grain boundary within a single domain is expected to change linearly with strain. Grain boundaries can thus in principle be treated the same way as grains, when it comes to strain effects, with the only difference being their initial strain state and initial T_{c}.

The strain sensitivity of the critical current of full-size coated conductors, expressed by the parameter a in equation (1), is likely determined by several factors besides the rate at which T_{c} changes with uniaxial pressure. A macroscopic current in coated conductors will run over many parallel and series current paths and cross many twin planes and grain boundaries. The alignment between the individual grains is not perfect, which causes the alignment between the strain and the a- and b-axes to vary locally within a few degrees. All these factors result in a summation of many rooftop-like patterns like the one outlined in the inset on the right in figure 4(a), with slight variations in slope and strain at which the peak occurs. This summation could result in a near parabolic strain dependence of I_{c} that is measured in all IBAD-MOCVD REBCO coated conductors, and the variations in strain sensitivity between conductors will thus be determined in part by variations in the texture of the conductor. Nevertheless, a key characteristic of such conductors is the general alignment of either a or b parallel to the wire axis.

The linear strain dependence of I_{c} that has been measured in ISD DBCO coated conductors is very different and can be explained by taking its crystallographic texture into account. The superconducting grains in ISD DBCO coated conductors (and others, such as ISD YBCO [42]) are aligned with their [110] direction parallel to the conductor axis [30]. Strain that is applied along the conductor axis will thus be oriented at a 45° angle with both the a- and b-axes (see figure 4(b)). The change in T_{c} with the deformation along the a-axis will be largely canceled by the opposite sign change in T_{c} with the deformation along the b-axis, and I_{c} will be almost insensitive to axial strain, independent of the presence of twin planes.

3.3. Anisotropic reversible strain effect in IBAD-MOCVD REBCO

As outlined in section 3.2, the difference in reversible strain dependence of I_{c} between IBAD-MOCVD and ISD REBCO coated conductors can be explained by the difference in in-plane orientation along the length of the conductor, and thus the orientation between the applied strain and the a- and b-axes of the superconducting film. A linear strain dependence of I_{c} can thus be expected in IBAD-MOCVD REBCO coated conductors when strain is applied at a 45° angle with respect to the conductor axis, parallel to the [110] direction of the superconducting film. Several bridges were patterned by laser in sections cut from IBAD-MOCVD sample S-3 to determine the existence of such an anisotropic in-plane reversible strain effect. The orientation of each bridge with respect to the axis of the coated conductor varies between 0° and 90° (see table 2), whereas the strain was always applied along the direction of the bridge.

Because of twinning, the superconducting lattice in IBAD-MOCVD REBCO coated conductors alternates the [100] and [010] directions along the length and across the width of the conductor. A similar strain dependence of I_{c} for bridges that are patterned at a nominal angle of 0° from the conductor axis (samples B-1 and B-2), and patterned at a nominal angle of 90° with respect to the conductor axis (samples B-10 to B-12), is expected. Such a comparable strain dependence of I_{c} is indeed measured, as is shown in figure 5(a), where the normalized critical currents for samples B-1 and B-10 are plotted as a function of applied strain. The strain dependence of I_{c} is fitted with equation (1), and the fitting parameters are listed in table 2. Unfortunately, only data for the bridges that were patterned at a nominal angle of 0° could be measured as a function of compressive strain, since the contact pads of samples B-1 and B-2 delaminated during the measurement. The change in I_{c} with strain is comparable for both samples and was fully reversible, which was confirmed by unloading the strain (open symbols). The strain dependence of the normalized I_{c} of bridges B-3 and B-7, that are oriented at an angle of 22.7° and 65.1° with respect to the conductor axis, is shown in figure 5(b). The strain sensitivity of I_{c} in these two samples is reduced by about 46% and 54%, respectively, compared to that of the sample with the highest strain sensitivity (B-11; see table 2), in which strain was oriented along the a- and b-axes.

The critical current of the bridges that were patterned at a nominal angle of 45° with respect to the conductor axis, along the [110] direction of the superconducting film, is almost independent of strain (see figure 5(c)). The strain sensitivity of I_{c} for samples B-5 and B-6, patterned at 44.7° and 47.4°, respectively, is only about 3% and 7% of that for sample B-11. The fact that I_{c} is still slightly dependent on strain is likely

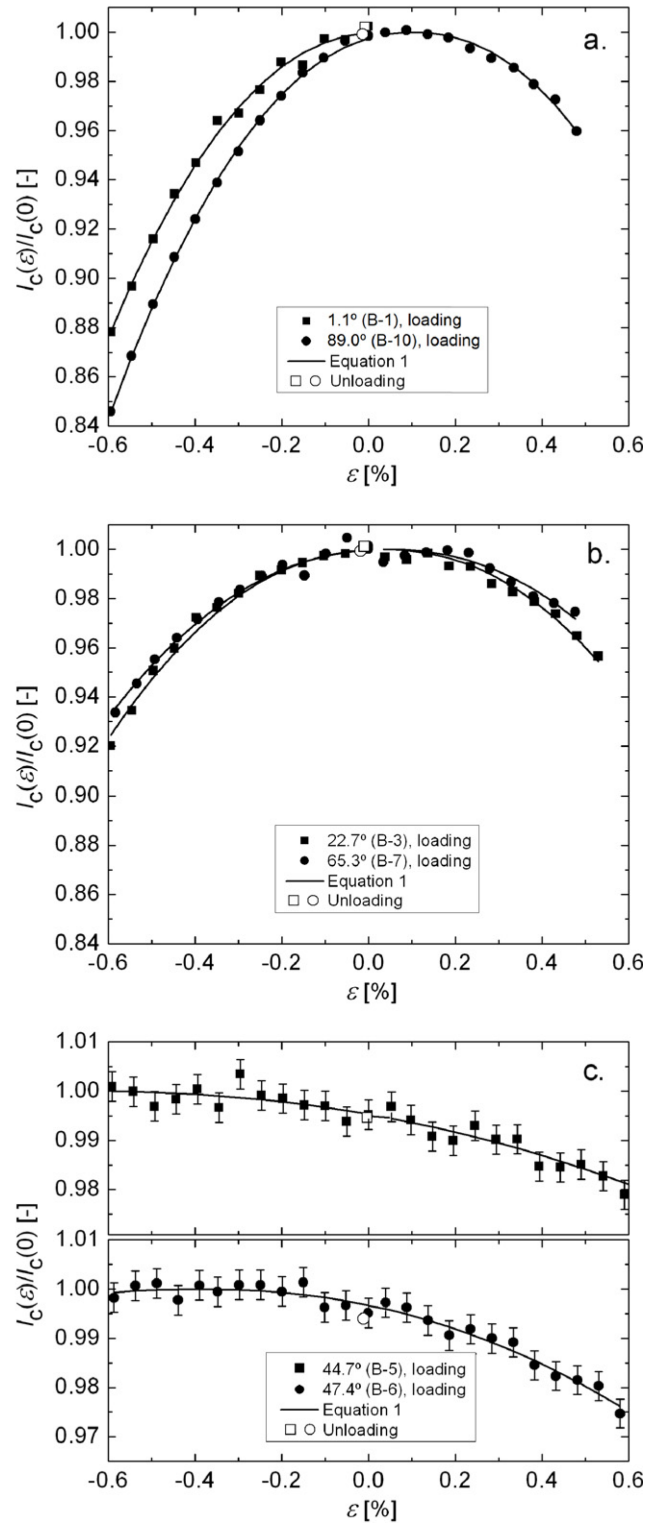

Figure 5. (a) Strain dependence of I_c at 76 K, normalized to its value at zero applied strain, of samples B-1 and B-10 that are oriented at 1.1° and 89.0° with the conductor axis, respectively. (b) Strain dependence of the normalized I_c of samples B-3 and B-7 that are oriented at 22.7° and 65.3° with the conductor axis, respectively. (c) Strain dependence of the normalized I_c of samples B-5 and B-6 that are oriented at 44.7° and 47.4° with the conductor axis, close to being parallel to the [110] direction of the superconducting film. The error bars indicate the ±0.3% uncertainty in I_c. All data were reversible, which was confirmed by unloading the strain (open symbols). The solid lines represent a fit to the data by use of equation (1).

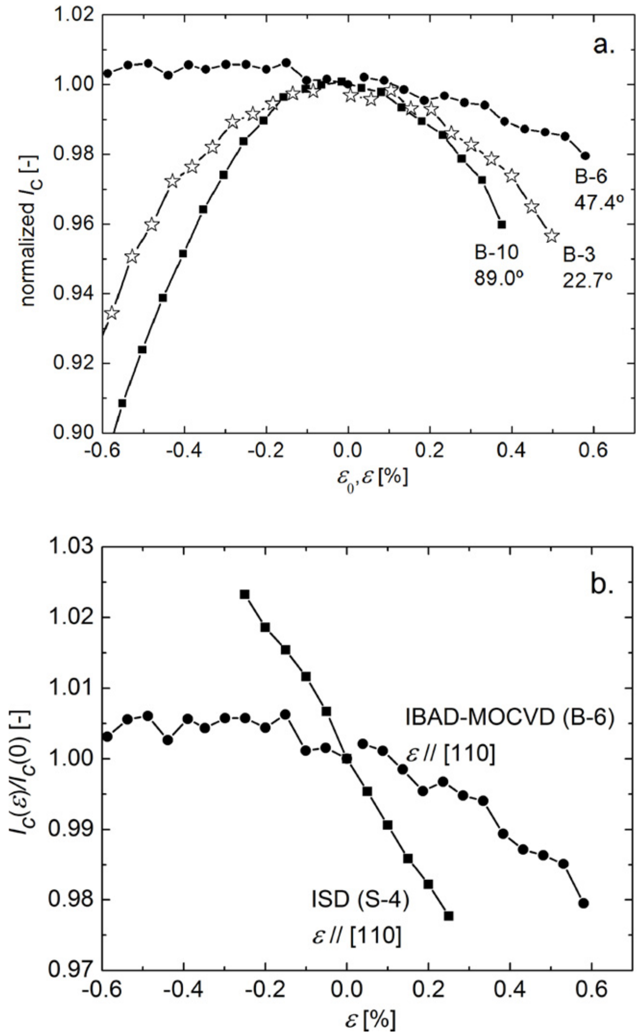

Figure 6. (a) Normalized I_c as a function of intrinsic strain ε_0 of samples B-3 and B-10 and as a function of applied strain for sample B-6 at 76 K, highlighting the change in strain sensitivity with in-plane strain orientation. The solid lines are a fit to the data with equation (1). (b) Comparison between the strain dependence of the normalized I_c of IBAD-MOCVD sample B-6 and ISD sample S-4 at 76 K.

caused by the small but finite in-plane grain misalignment in the coated conductor, and by the ±2.5° uncertainty in the alignment between the applied strain and the [110] direction of the film. The strain (ε_m) at which the peak in I_c occurs is −0.67% for sample B-5 and −0.39% for sample B-6, which is at a much higher compressive strain than that of the other bridges, where ε_m is between 0.02% and 0.1%. It is likely that ε_m is determined by other factors beside the initial strain state of the superconducting film, which is a conclusion similar to that drawn when investigating the reversible strain effect as a function of temperature and in the presence of a magnetic field [17, 43]. Finally, the strain dependence of the normalized critical current of sample B-10 (89.0°), sample B-3 (22.7°) and sample B-5 (44.7°) are compared in figure 6(a) to clearly demonstrate the highly anisotropic nature of the in-plane reversible strain effect in IBAD-MOCVD coated conductors.

Differences in strain sensitivity of I_c exist between the IBAD-MOCVD bridges and the ISD coated conductor when, in both cases, strain is applied along the [110] direction of the superconducting film. The small strain dependence of I_c that remains in IBAD-MOCVD sample B-6 is much lower than the strain sensitivity of I_c for ISD sample S-4 (see figure 6(b)). The higher, linear strain sensitivity of I_c measured in ISD DBCO sample S-4 is likely caused by its much broader in-plane grain misorientation, besides a possible difference in pressure dependence of T_c in DBCO, compared to YGBCO. For instance, the c-axis in MOCVD IBAD YGBCO is oriented normal to the substrate, while the c-axis in ISD DBCO is tilted sideways by a relatively large angle [44]. A fully three-dimensional strain investigation has to be performed for us to fully understand the differences between the strain dependences of I_c in the two types of coated conductors.

The anisotropic nature of the pressure dependence of T_c in REBCO causes the strain sensitivity of I_c to depend on the in-plane strain orientation. The strain sensitivity parameter $a(\alpha)$ of the patterned bridges is proportional to the change in T_c with strain, since differences in microstructure between bridges patterned from the same section of coated conductor are expected to be negligible:

$$a(\alpha) \approx \frac{\mathrm{d}T_c}{\mathrm{d}\varepsilon} = \varepsilon\cos(\alpha)\frac{\mathrm{d}T_c}{\mathrm{d}\varepsilon_a} + \varepsilon\sin(\alpha)\frac{\mathrm{d}T_c}{\mathrm{d}\varepsilon_b}. \qquad (5a)$$

The strain component parallel to the a-axis is defined as ε_a and the component parallel to the b-axis is defined as ε_b. The small change in T_c with strain along the c-axis is neglected in this approximation, because the strain is applied within the ab-plane. Since $\mathrm{d}T_c/\mathrm{d}\varepsilon_a$ and $\mathrm{d}T_c/\mathrm{d}\varepsilon_b$ in REBCO are equal, but of opposite sign [22], equation (5a) can be simplified to

$$a(\alpha) = a(0°)|\cos(\alpha) - \sin(\alpha)| \qquad (0° \leqslant \alpha \leqslant 90°). \quad (5b)$$

Parameter $a(0°)(=a(90°))$ is the maximum strain sensitivity that occurs when the applied strain is oriented parallel to the [100] and [010] directions of the superconducting film. The expected angular dependence of $a(\alpha)$, according to equation (5b), with $a(0°) = 7985$ as the average value of a for samples B-1, B-2, B-10 and B-11, is plotted in figure 7. The strain sensitivity of I_c for each bridge obtained from experiments is included in the figure. A good agreement between the model and data is obtained, except for sample B-11. The strain sensitivity of I_c of samples B-1, B-2 (at 1.1° and 1.0°, respectively) and B-10 (at 89.0°) is between 7647 and 7744, while that of sample B-11 (at 88.2°) is much higher at 8866 (see table 2). This relatively large difference can be explained by a small defect in the bridge of sample B-11, which was observed with magneto-optical imaging (see figure 5(a)). Stress concentrations around this defect likely cause a higher strain sensitivity of I_c, although the defect is small enough not to reduce the overall I_c of the bridge.

An anisotropic in-plane reversible strain effect is highly likely to be present in other types of coated conductors besides IBAD-MOCVD. The strain dependence of I_c in ISD DBCO is expected to become a power-law function when strain is applied at 45° to the tape axis along the [100] and [010] directions of the DBCO film. The power-law dependence could potentially be asymmetric with respect to its peak, due

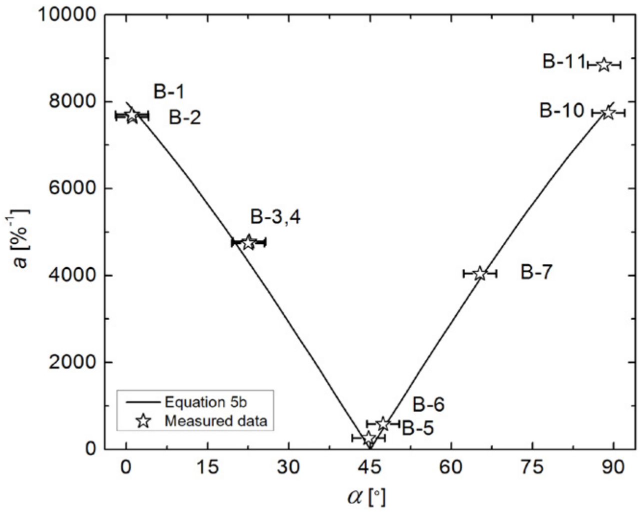

Figure 7. The strain sensitivity parameter $a(\alpha)$ is plotted as a function of angle α between the applied strain and the [100] and [010] directions of the superconducting film. The error bars of ±2.5° include the uncertainty in the orientation of the patterned bridges with the conductor axis and the uncertainty in alignment between the applied strain and the bridge. The solid line is the expected angular dependence of $a(\alpha)$, expressed by equation (5b).

to the relatively high slope of the linear I_c versus strain dependence when strain is aligned with [110]. Also, a power-law, reversible strain dependence of I_c similar to that in IBAD-MOCVD coated conductors has been measured in coated conductors prepared by metal–organic deposition (MOD) on rolling assisted biaxially textured substrates (RABiTS), and those prepared by pulsed-laser deposition (PLD) on IBAD substrates [19, 45, 46]. A strain independent-I_c is expected in these conductors when the strain is applied along the [110] direction of the superconducting film.

The anisotropic in-plane reversible strain effect in IBAD-MOCVD coated conductors reported here has significant implications for REBCO coated conductors. For instance, the critical current of IBAD-MOCVD coated conductors that are wound into compact cables is determined mainly by the strain component along the axis of the conductor, and not by the maximum strain component [47]. In some cable configurations, the critical current remained almost unchanged, even though the conductors experienced a significant compressive strain [37]. Since the strain applied to the IBAD-MOCVD coated conductor in this particular cable configuration turns out to be oriented close to 45° from the conductor axis, the principal strain then lies along the [110] direction of the superconducting film. Cables wound from ISD DBCO coated conductors in this particular cable configuration would thus be expected to show a much larger reversible degradation in I_c due to cabling, since the resulting cabling strain occurs at 45° to the conductor axis and is thus oriented along the [100] and [010] directions of the superconducting film. This hitherto unknown strain effect in coated conductors thus has an important and, for modern IBAD-MOCVD conductors, a very positive effect on twisted cables.

4. Conclusions

For the first time, we have established a qualitative correlation between the uniaxial pressure dependence of the critical temperature and the reversible strain effect on the critical current in high-temperature superconducting REBCO coated conductors. An anisotropic in-plane reversible strain effect on the critical current in IBAD-MOCVD REBCO coated conductors was discovered. The maximum strain sensitivity of the critical current occurs when the applied strain is aligned with the [100] and [010] directions of the superconducting film, and the critical current becomes almost insensitive to strain when the strain is aligned with the [110] direction. This effect has been directly correlated to the uniaxial pressure dependence of the critical temperature, which is highly anisotropic in REBCO superconductors. The effect has important implications for the application of coated conductors, especially in compact cables.

Acknowledgments

The authors thank Dr Sugano and Professor Awaji for technical discussions and SuperPower Inc. for providing the IBAD-MOCVD coated conductor in which the bridges were patterned. This work at NIST and at FSU was supported in part by the US Department of Energy, Office of Electricity Delivery and Energy Reliability.

References

[1] Ekin J W, Finnemore D K, Li Q, Tenbrink J and Carter W 1992 *Appl. Phys. Lett.* **61** 858–60
[2] ten Haken B, ten Kate H H J and ten Brink J 1995 *IEEE Trans. Appl. Supercond.* **5** 1298–301
[3] Kitaguchi H, Itoh K, Kumakura H, Takeuchi T, Togano K and Wada H 2001 *IEEE Trans. Appl. Supercond.* **11** 3058–61
[4] van der Laan D C, Ekin J W, van Eck H J N, Dhalle M, ten Haken B, Davidson M W and Schwartz J 2006 *Appl. Phys. Lett.* **88** 022511
[5] ten Haken B, Beuink A and ten Kate H H J 1997 *IEEE Trans. Appl. Supercond.* **7** 2034–7
[6] Kovac P and Bukva P 2001 *Supercond. Sci. Technol.* **14** L8–11
[7] Passerini R, Dhallé M, Seeber B and Flükiger R 2002 *Supercond. Sci. Technol.* **15** 1507–11
[8] Sugano M, Osamura K and Nyilas A 2004 *Physica* C **412** 1114–9
[9] van der Laan D C, Douglas J F, Clickner C C, Stauffer T C, Goodrich L F and van Eck H J N 2011 *Supercond. Sci. Technol.* **23** 032001
[10] Garcia-Moreno F, Usoskin A, Freyhardt H C, Wiesmann J, Dzick J, Heinemann K and Hoffmann J 1997 *Inst. Phys. Conf. Ser.* **158** 1093–6
[11] Cheggour N, Ekin J W, Clickner C C, Verebelyi D T, Thieme C L H, Feenstra R and Goyal A 2003 *Appl. Phys. Lett.* **83** 4223–5
[12] Sugano M, Osamura K, Prusseit W, Semerad R, Itoh K and Kiyoshi T 2005 *IEEE Trans. Appl. Supercond.* **15** 3581–5
[13] Cheggour N, Ekin J W, Thieme C L H, Xie Y Y, Selvamanickham V and Feenstra R 2005 *Supercond. Sci. Technol.* **18** S319–24
[14] Uglietti D, Seeber B, Abacherli V, Carter W L and Flükiger R 2006 *Supercond. Sci. Technol.* **19** 869–72
[15] van der Laan D C and Ekin J W 2007 *Appl. Phys. Lett.* **90** 052506
[16] Sugano M, Nakamura T, Manabe T, Shikimachi K, Hirano N and Nagaya S 2008 *Supercond. Sci. Technol.* **21** 115019
[17] van der Laan D C, Ekin J W, Douglas J F, Clickner C C, Stauffer T C and Goodrich L F 2010 *Supercond. Sci. Technol.* **23** 072001
[18] van der Laan D C, Haugan T J and Barnes P N 2009 *Phys. Rev. Lett.* **103** 027005
[19] van der Laan D C, Haugan T J, Barnes P N, Abraimov D, Kametani F, Larbalestier D C and Rupich M W 2010 *Supercond. Sci. Technol.* **23** 014004
[20] Villaume A, Antonevici A, Bourgault D, Porcar L, Leggeri J P and Villard C 2007 *Supercond. Sci. Technol.* **20** 1019–25
[21] Antonevici A and Villard C 2008 *Supercond. Sci. Technol.* **21** 075002
[22] Welp U, Grimsditch M, Fleshler S, Nessler W, Downey J, Crabtree G W and Guimpel J 1992 *Phys. Rev. Lett.* **69** 2130–3
[23] Chen X F, Tessema G X and Skove M J 1991 *Physica* C **181** 340
[24] Kierspel H, Winkelmann H, Auweiler T, Schlabitz W, Büchner B, Duijn V H M, Hien N T, Menovsky A A and Franse J J M 1996 *Physica* C **262** 177
[25] Meingast C, Junod A and Walker E 1996 *Physica* C **272** 106
[26] Selvamanickam V 2001 *IEEE Trans. Appl. Supercond.* **11** 3379–82
[27] Selvamanickam V, Xie Y Y, Reeves J and Chen Y 2004 *MRS Bull.* **29** 579–82
[28] Osamura K, Machiya S, Tsuchiya Y and Suzuki H 2010 *Supercond. Sci. Technol.* **23** 045020
[29] Prusseit W, Nemetschek R, Hoffmann C, Sigl G, Lumkemann A and Kinder H 2005 *Physica* C **426** 866–71
[30] Sugano M 2010 private communication
[31] Feldmann D M *et al* 2000 *Appl. Phys. Lett.* **77** 2906–8
[32] van der Laan D C, Dhallé M, Naveira L M, van Eck H J N, Metz A, Schwartz J, Davidson M W, ten Haken B and ten Kate H H J 2005 *Supercond. Sci. Technol.* **18** 299–306
[33] van der Laan D C, Dhallé M, van Eck H J N, Metz A, ten Haken B, ten Kate H H J, Naveira L M, Davidson M W and Schwartz J 2005 *Appl. Phys. Lett.* **86** 032512
[34] Abraimov D, Feldmann D M, Polyanskii A A, Gurevich A, Daniels G, Larbalestier D C, Zhuravel A P and Ustinov A V 2004 *Appl. Phys. Lett.* **85** 2568–70
[35] Abraimov D V, Feldmann D M, Polyanskii A A, Gurevich A, Liao S, Larbalestier D C, Zhuravel A P and Ustinov A V 2005 *IEEE Trans. Appl. Supercond.* **15** 2954–7
[36] Sugano M, Choi S, Miyazoe A, Miyamatsu K, Ando T, Itoh K, Kiyoshi T, Wada H and Selvamanickam V 2008 *IEEE Trans. Appl. Supercond.* **18** 1143–6
[37] van der Laan D C, Lu X F and Goodrich L F 2011 *Supercond. Sci. Technol.* **24** 042001
[38] Safar H, Foltyn S, Kung H, Maley M P, Willis J O, Arendt P and Wu X D 1996 *Appl. Phys. Lett.* **68** 1853–5
[39] Osamura K, Machiya S, Tschuchiya Y, Harjo S, Suzuki H, Shobu T, Kiriyama K and Sugano M 2011 *IEEE Trans. Appl. Supercond.* **21** 3090–3
[40] Neuhaus W and Winzer K 1992 *Cryogenics* **32** 357–61
[41] Goyal A, Oliver W C, Funkenbusch P D, Kroeger D M and Burns S J 1991 *Physica* C **183** 221–33
[42] Sugano M, Osamura K, Prusseit W, Semerad R, Itoh K and Kiyoshi T 2005 *Supercond. Sci. Technol.* **18** S344–50
[43] Sugano M, Shikimachi K, Hirano N and Nagaya S 2010 *Supercond. Sci. Technol.* **23** 085013
[44] Bauer M, Metzger R, Semerad R, Berberich P and Kinder H 2000 *Mater. Res. Soc. Symp.* **585** 35–44
[45] Palau A, Puig T, Obradors X, Feenstra R and Freyhardt H C 2005 *IEEE Trans. Appl. Supercond.* **15** 2790–3
[46] Shin H S, Dizon J R C, Ko R K, Kim T H, Ha D W and Oh S S 2007 *Physica* C **463** 736–41
[47] van der Laan D C 2009 *Supercond. Sci. Technol.* **22** 065013